

Dynamic shear strength of unreinforced and Hairpin-reinforced cast-in-place anchors using shaking table tests

Dong Hyun Kim¹, Yong Myung Park^{*1}, Choong Hyun Kang² and Jong Han Lee³

¹Department of Civil Engineering, Pusan National University, Busan, 46241, Republic of Korea

²Seismic Simulation Test Center, Pusan National University, Busan, 46241, Republic of Korea

³Department of Civil Engineering, Daegu University, Gyeongsbuk, 38453, Republic of Korea

(Received August 7, 2015, Revised December 25, 2015, Accepted January 11, 2016)

Abstract. Since the publication of ACI 318-02, the concrete capacity design (CCD) method has been used to determine the resistance of unreinforced concrete anchors. The regulation of steel-reinforced anchors was proposed in ACI 318-08. Until ACI 318-08, the shear resistance of concrete breakout for an unreinforced anchor during an earthquake was reduced to 75% of the static shear strength, but this reduction has been eliminated since ACI 318-11. In addition, the resistance of a hairpin-reinforced anchor was calculated using only the strength of the steel, and a regulation on the dynamic strength was not given for reinforced anchors. In this study, shaking table tests were performed to evaluate the dynamic shear strength of unreinforced and hairpin-reinforced cast-in-place (CIP) anchors during earthquakes. The anchors used in this study were 30 mm in diameter, with edge distances of 150 mm and embedment depths of 240 mm. The diameter of the hairpin steel was 10 mm. Shaking table tests were carried out on two specimens using the artificial earthquake, based on the United States Nuclear Regulatory Commission (US NRC)'s Regulatory Guide 1.60, and the Northridge earthquake. The experimental results were compared to the current ACI 318 and ETAG 001 design codes.

Keywords: cast-in-place anchor; unreinforced anchor; hairpin-reinforced anchor; dynamic shear strength; shaking table tests

1. Introduction

Anchors in concrete are of great importance in the connection and support of structural elements and equipment. In general, large steel columns and facilities are connected to concrete structures using cast-in-place (CIP) anchors which are installed before placing concrete. Anchors play very important roles during earthquakes because they affect the safety of the entire structure and the components of the structure connected to the anchors. Furthermore, an increase in the frequency of earthquakes focuses attention on the resistance of anchors in concrete under seismic loading. For structures such as energy and power plants in particular, the anchor-connected components must have sufficient seismic resistance.

The behavior of concrete anchors during earthquakes depends mainly on the shear loading.

*Corresponding author, Professor, E-mail: ympk@pusan.ac.kr

Until the publication of the American Concrete Institute's ACI 318-08 (ACI Committee 318 2008) design code, the design strength of the anchor required an additional reduction factor of 0.75 for both tensile and shear strength in moderate and strong seismic regions. This requirement was intended to induce ductile failure in steel anchors and ensure a safe concrete breakout strength during an earthquake. The requirement was also attributable to the lack of experimental data related to the concrete breakout strength under dynamic loading. The 2011 revision, ACI 318-11 (ACI Committee 318 2011) retained the factor of 0.75 for the tensile loading. But, the reduction factor for the shear loading was removed without a reason being provided, and this revised specification remained in ACI 318-14 (ACI Committee 318 2014).

ACI 318-08 specified steel reinforcement for concrete anchors for cases in which the plastic breakout strength of the concrete is less than the ductile failure strength of a steel anchor. The concrete breakout strength can be replaced by the resistance of the steel reinforcement of the reinforced anchor but not by the summation of the concrete strength and steel reinforcement strength. For dynamic loading, neither ACI 318-08 nor ACI 318-14 provide an additional requirement for steel reinforcement. This means that shear strength reinforced with steel can be evaluated in terms of the steel resistance, regardless of the static and dynamic loads. The European guideline for metal anchors in concrete, ETAG 001 (2012), proposes an equation for the concrete breakout strength that is similar to that in ACI 318-08. However, ETAG 001 does not identify a strength reduction factor for dynamic loading, which suggests that the dynamic breakout strength is considered to be identical to the static breakout strength.

Previous experimental research (Eligehausen *et al.* 2006, Klingner *et al.* 1982, Gross *et al.* 2001) on the static shear strength of hairpin-reinforced anchors, i.e., anchors reinforced with hairpin-shape steel bar, has been very limited. Furthermore, few studies have been conducted on the evaluation of the dynamic shear resistance of hairpin anchors, particularly CIP anchors, using seismic waves. Therefore, this experimental study was carried out to evaluate the shear resistance of hairpin-reinforced anchors under seismic loading. ACI 318-11 and ETAG 001 require evaluation of seismic performance using seismic qualification testing for post-installed (PI) anchors which are installed in hardened concrete but not for CIP anchors. Therefore, most studies on the subject have focused on the dynamic performance of PI anchors under cyclic loading. However, there are differences among the relevant design standards (ETAG 001 2012, ACI 355.2 2000, CSA N287.2 1998) concerning the shape, magnitude, and frequency of the cyclic loading to be used for seismic qualification testing. Furthermore, few studies have been conducted on the shear resistance of CIP anchors using actual earthquake waves. Therefore, the dynamic shear resistance of CIP anchors and the influence of hairpin reinforcement on shear strength was evaluated in this study using shaking table tests.

2. Previous research and design codes

2.1 Previous research

Eligehausen *et al.* (2006) reported the test results of the static shear resistance of unreinforced and reinforced 22-mm-diameter anchors. The results are shown in Fig. 1 (Curve ①: unreinforced anchor, Curve ②: stirrup-reinforced anchor, Curves ③ and ④: stirrup-reinforced and 12-mm-diameter hairpin-reinforced anchor). According to Fig. 1, compared to the maximum strength of the anchor with hairpin reinforcement in direct contact with the anchor shaft (Curve ④), that of

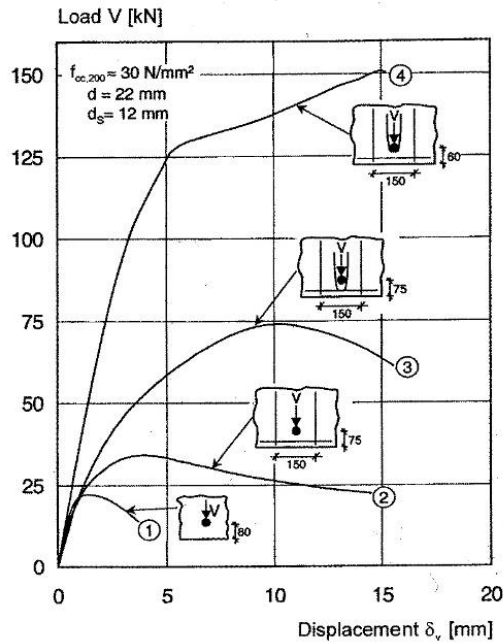


Fig. 1 Effect of reinforcement on the behavior of single anchor (Eligehausen *et al.* 2006)

the anchor with hairpin reinforcement away from the anchor shaft (Curve ③) was significantly reduced due to the compressive failure of the concrete between the anchor shaft and the hairpin. The researchers also suggested that the shear strength of the anchor decreases as the cover of the hairpin reinforcement increases because the deformation of the anchor increases, demonstrating the restraining effect of the hairpin reinforcement on the anchor. Klingner *et al.* (1982) performed tests on 19-mm-diameter anchors under quasi-statically monotonic and reversed cyclic shear and evaluated the effect of the cover and contact of the hairpin reinforcement on the shear strength. According to the result, the strength was higher when the hairpin reinforcement was in direct contact with the anchor shaft and close to the surface of the concrete.

To assess the dynamic resistance of anchors, Gross *et al.* (2001) carried out experiments on unreinforced and hairpin-reinforced CIP anchors 19 mm in diameter in an uncracked concrete block. The dynamic load applied in the study was a ramp loading with a 0.1-second rising time. From the test results, the static resistance of a hairpin-reinforced anchor was 1.43 times greater than that of an unreinforced anchor, and the dynamic strength was 1.27 and 1.21 times greater than the static resistance of an unreinforced and hairpin-reinforced anchor, respectively. The dynamic strength being higher than the static strength might be attributable to the strain-rate effect of the ramp loading in the form of impact loading. Petersen *et al.* (2013) carried out experiments on 19-mm-diameter CIP anchors in plain concrete under quasi-static monotonic and cyclic shear loadings. No differences in the concrete breakout strength were observed under uni-cyclic versus reversed cyclic shear loadings. In addition, no strength reduction, compared with the strength measured in quasi-static monotonic shear load testing, was detected. Park *et al.* (2014) attempted to evaluate the dynamic strength of hairpin-reinforced anchors in uncracked concrete using 1-Hz pulsating cyclic loading. The results of the study showed that the strength of hairpin-reinforced

anchors was considerably greater than that of unreinforced anchor. There was also no decrease in the shear strength of the anchor, compared with the static strength, under a dynamic pulsating load.

Very little research has been conducted on the static and dynamic strength of hairpin-reinforced anchors under shear loading. A few studies of the strength of hairpin-reinforced anchors under seismic loading have been carried out using impact loading, which is different from evaluation of the strength under seismic loading because of the loading pattern and the strain-rate effect. No studies related to unreinforced and reinforced anchors in real earthquakes are known to have been conducted.

2.2 Design codes for shear strength of concrete anchor

2.2.1 ACI 318 code

Based on the concrete capacity design (CCD) method, the American Concrete Institute's design code ACI 349-01 (ACI Committee 349 2001) and ACI 318-02 (ACI Committee 318 2002) proposed a 5% fractile strength for the design of concrete breakout strength of anchors in cracked concrete. In this study, the proposed equation was expressed as the average breakout strength of uncracked concrete for purposes of comparison with the experimental results. The following equation gives the average concrete breakout strength of an anchor in uncracked concrete under static shear loading

$$V_{ACI318-02} = 1.1 \left(\frac{l_e}{d_o} \right)^{0.2} \sqrt{d_o} \sqrt{f_{ck}} c_{a1}^{1.5} (N) \quad (1)$$

where d_o =the anchor diameter (mm); l_e =the load-bearing length, limited to a maximum of $8d_o$ (mm); c_{a1} =the edge distance (mm); and f_{ck} =the compressive strength of cylindrical specimens (MPa). Lee *et al.* (2010) indicated that as the edge distance increases, the concrete breakout strength calculated using Eq. (1) increasingly overestimates the actual strength. Therefore, they proposed a modified equation that excluded the effect of anchor diameter and load-bearing length. ACI 318-11 included the equation proposed by Lee *et al.*, shown as Eq. (2), and defined the concrete breakout strength as the smaller of the two strength values calculated using Eqs. (1)-(2).

$$V_{ACI318-11} = 7.0 \sqrt{f_{ck}} c_{a1}^{1.5} (N) \quad (2)$$

For dynamic shear loading, as previously described, the concrete breakout strength required was determined by decreasing by 25% the static shear strength calculated using Eq. (1) until ACI 318-08, but the revision of ACI 318-11 deleted this strength reduction factor. In addition, ACI 318-08 proposed a standard for hairpin-reinforced anchors. According to this standard, hairpin steel should adhere to the anchor shaft and be installed as close as possible to the concrete surface, as shown in Fig. 2. The steel development length also has to be secured from the failure section. The concrete breakout strength can then be replaced by the steel resistance strength. The design strength of the reinforced anchor can be calculated as follows

$$\phi V_{ACI318}^{reinf.} = \phi A_{se} f_y \quad (3)$$

where ϕ =the strength reduction factor of 0.75 for reinforcement, A_{se} =the effective section of the reinforcement (mm^2), and f_y =the yield strength of the reinforcement (MPa).

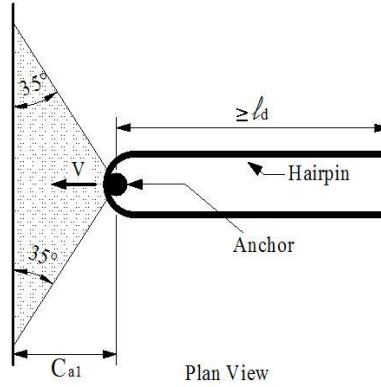


Fig. 2 Hairpin reinforcement

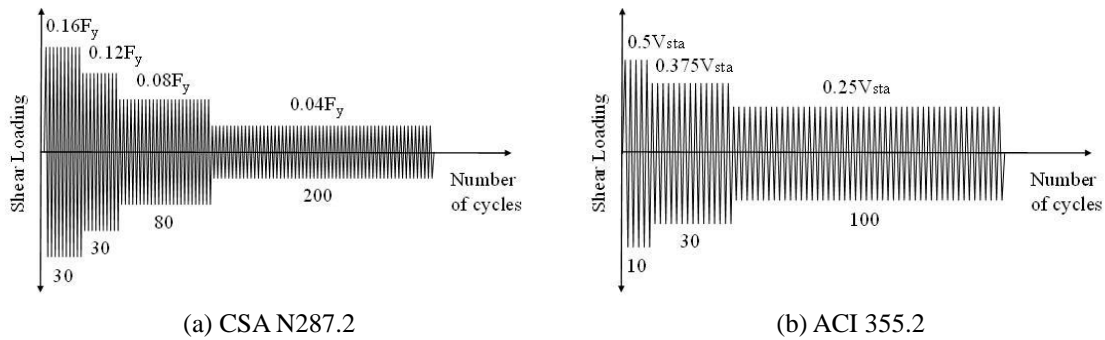


Fig. 3 Cyclic loading for seismic qualification tests

2.2.2 ETAG 001 Code

Based on the results presented by Eligehausen and Hofmann (2003), The European ETAG 001 (2012) standard provided Eq. (4) for calculation of the concrete breakout strength

$$V_{ETAG001} = k d_o^{\alpha} l_e^{\beta} \sqrt{f_{cc}} c_{a1}^{1.5} (N) \quad (4)$$

where $\alpha = 0.1 \left(\frac{l_e}{c_{a1}} \right)^{0.5}$, $\beta = 0.1 \left(\frac{d_o}{c_{a1}} \right)^{0.2}$, and f_{cc} = the concrete compressive strength of cubic specimens (MPa), and $k=2.4$ for uncracked concrete in ETAG 001 ($k=3.0$ for mean strength). The CCD theory on which the European and American standards are based for the concrete breakout strength, but the two standards take the effects of the anchor diameter and load-bearing length into account in different ways. For dynamic shear loading, ETAG 001 does not provide an additional strength reduction factor, which means that the dynamic breakout strength is considered to be the same as the static breakout strength. In addition, unlike the American standard, ETAG 001 has no requirements concerning the hairpin reinforcement for anchors in concrete.

2.3 Codes for seismic qualification testing

The purpose of this study is to evaluate the shear resistance of anchors using shaking table tests. The shape and frequency of the seismic wave was determined based on the seismic

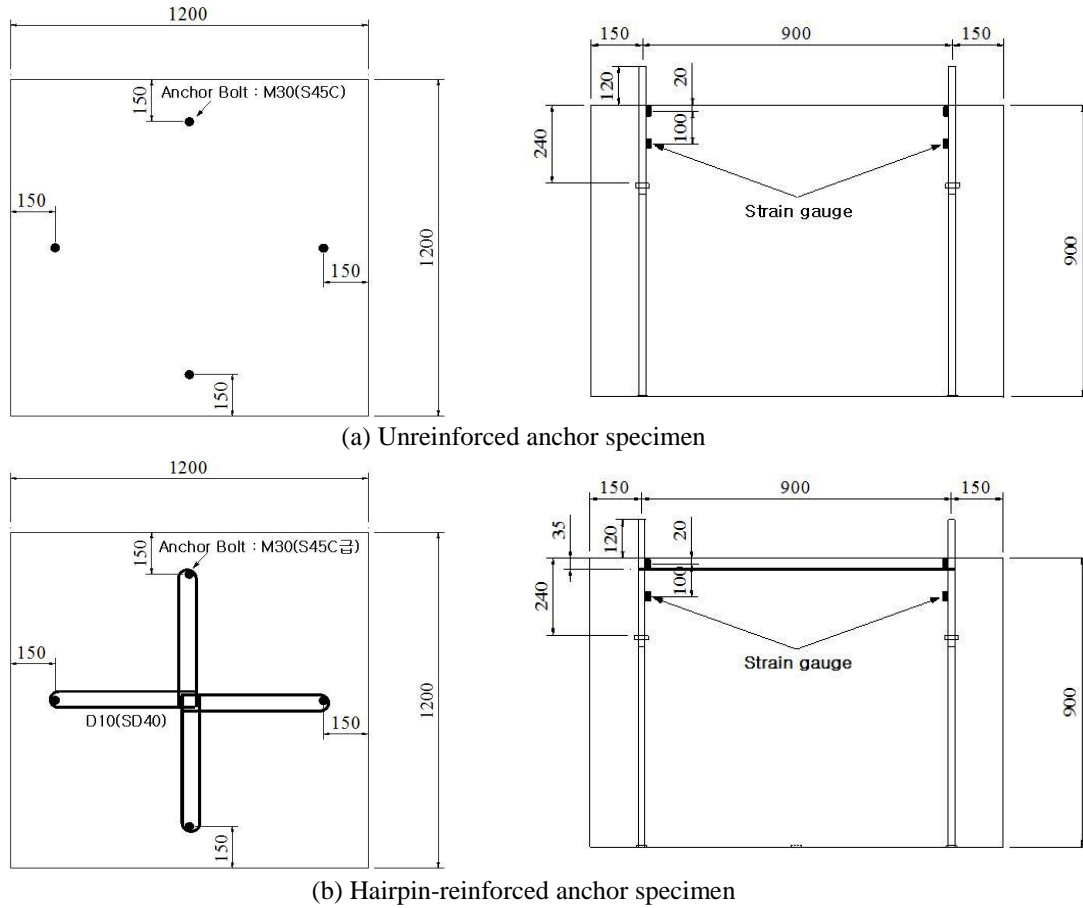


Fig. 4 Anchor specimens for the shaking table tests (Units: mm)

qualifications of CSA N287.2 and ACI 355.2. The difference is that CSA N287.2 aims at evaluating the fatigue strength of anchor shaft used in the structure of nuclear power plants and ACI 355.2 evaluating the concrete strength of anchors. As shown in Fig. 3(a), CSA N287.2 applies the cyclic loading producing the shear stress of anchor shaft from $\pm 0.16F_y$ to $\pm 0.04F_y$ (F_y : the yielding stress of anchor steel) at a rate of 5-Hz. After a total of 340 cycle loadings, the static loading is applied until the failure. On the other hand, ACI 355.2 applies a total of 140 cycles of repeated loading with the magnitude from $\pm 0.5V_{sta}$ to $\pm 0.25V_{sta}$ (V_{sta} : the static breakout strength) at less than 2-Hz and after that, the shear static load is applied until the failure.

3. Testing program

3.1 Experimental program

The anchor type used in this study was an M30-S45C (yield strength $F_y=490$ MPa). Because ductile failure, i.e., shear failure of the anchor, is more likely to occur as the edge distance

increases, the edge distance and anchor embedment length were designed to induce concrete breakout failure. The required edge distance was determined to be 150 mm, as shown in Fig. 4, which is five times the anchor diameter considered to be the minimum for the anchor edge distance. The embedment depth of the anchor was determined to be 240 mm ($=8d_0$).

The size of the concrete specimen was 1200 mm×1200 mm×900 mm, and the design strength of the concrete was 27 MPa. Two concrete blocks, one with no reinforcement and the other with hairpin reinforcement 10 mm in diameter, with a bending radius of 40 mm and a cover depth of 35 mm. Each block had four anchors installed, so the seismic tests were performed eight times in total. For comparison with static shear strengths, specimens of the same size were also cast for unreinforced and hairpin-reinforced anchors.

3.2 Test setup

To evaluate the dynamic strength under earthquake loading, testing was carried out on a shaking table, as shown in Fig. 5. To introduce an inertia motion to the test specimen, roller guides (linear motion or LM guide) were installed between the floor plate and support plate. The anchor specimen was mounted on the floor plate and connected to the support frame via shear jig. To prevent the specimen from moving during the seismic testing, four columns (H-150×150×7×10) were installed, two in front of and two behind the specimen, and fixed to the floor plate using high-strength bolts. On both sides of the specimen, mass blocks were constructed on the floor plate, using ten steel blocks on each side. The weight of the mass block was determined to satisfy the range of frequency between 2 and 5 Hz (close to 3 and 4 Hz), which is almost the same range of the exciting frequency given in CSA N287.2 and ACI 355.2 standards. In addition, the natural frequency at the equipment support is mostly within the range of 2-5 Hz.

To evaluate the dynamic load applied to the anchor during the shaking table test, a load cell was installed between the shear jig and the support frame. The displacement was measured using a linear variable differential transducer (LVDT) installed on the back side of the shear jig, as shown in Fig. 6(a). To determine the exact moment of the concrete fracture, two strain gauges were installed at the left and right sides of the anchor as close as possible to the anchor on the top surface of the concrete specimen (see Fig. 6(a)). Fig. 6(b) shows the strain gauges installed on a hairpin before placement of the concrete. Two other strain gauges were installed on the anchor shaft, 20 mm and 120 mm below the concrete surface, as shown in Fig. 4. Accelerometers

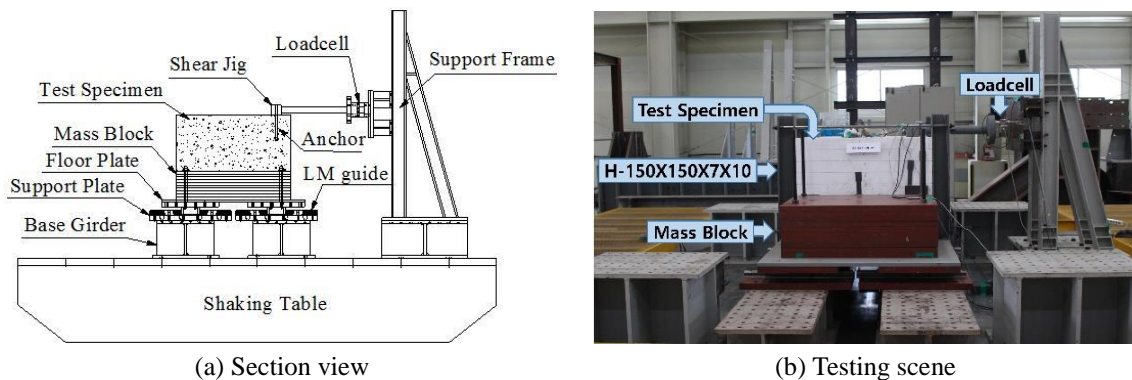


Fig. 5 Configuration of the shaking table test

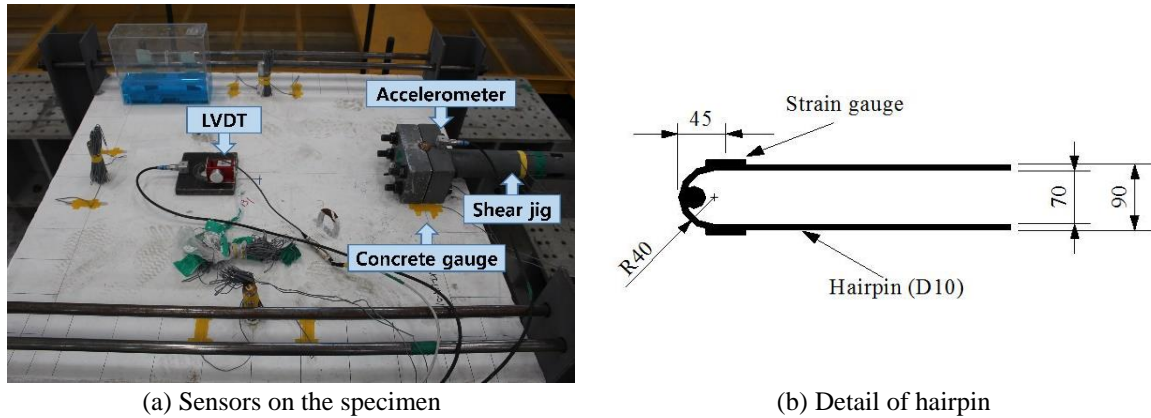


Fig. 6 Installation of anchors and instrumentation of sensors

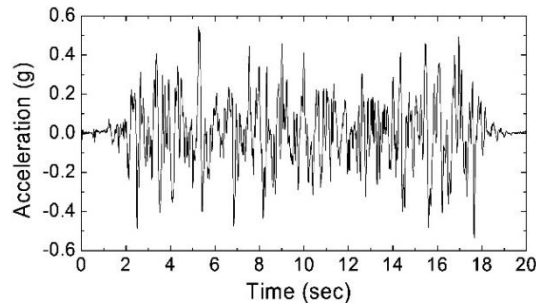
were installed on the top surface of the concrete block and the shaking table to measure the seismic loading response. The experimental data were acquired at a sampling rate of 512 Hz. Meanwhile, static shear tests were performed via monotonic loading using a universal testing machine (UTM).

3.3 Seismic loads

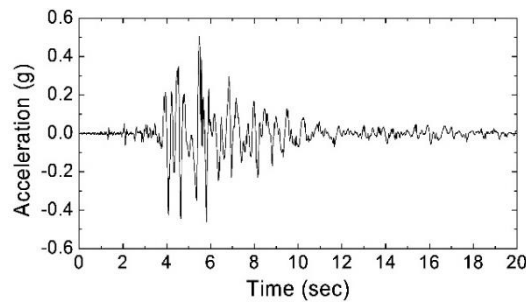
When evaluating the resistance of anchors under an earthquake, CSA N 287.2 and ACI 355.2 specify a different number of excitation, as described in Fig. 3. Thus, this study used two types of earthquakes; an artificial earthquake based on the design response spectrum of the United States Commission (US NRC)'s Guide 1.60 (1973) and a real record for the Northridge earthquake, which produced large damages to concrete anchors.

The US NRC design response spectrum, obtained from probabilistic seismic risk analysis of 14 strong earthquakes in the western region of the US, was proposed to determine the input earthquake acceleration for the seismic design of a nuclear power plant. Fig. 7(a) shows the artificial earthquake, with a peak ground acceleration (PGA) of 0.5 g, created using the design response spectrum of US NRC Guide 1.60. The Northridge earthquake record was obtained from measurements obtained in the Newhall region, approximately 20 Km north of the epicenter. Fig. 7(b) shows the time history of the seismic acceleration measured at Newhall. The duration of the seismic wave was set to be 20 seconds for both the artificial and Northridge earthquakes, as shown in Fig. 7. The earthquake generated from the US NRC Reg. Guide 1.60 includes lots of high peaks (strong seismic acceleration) for almost the entire duration of the seismic wave, while the Northridge earthquake shows relative small number of high peaks for approximately 4 to 6 seconds. Thus, in this study, the two types of earthquakes were used to differentiate the fracture mode of unreinforced and hairpin-reinforced anchors concerning the difference in the high peaks (strong seismic acceleration).

The PGA of the seismic wave used in the shaking table tests was gradually increased until failure of the specimen occurred. The initial PGA of the seismic test was set to be 0.2g, and the PGA was increased in increments of 0.05g until concrete breakout failure or anchor failure occurred. After application of a seismic wave, crack initiation and propagation in the concrete specimen were examined before application of the next seismic wave at a PGA 0.05g higher.



(a) Artificial earthquake from the US NRC 1.60 design response spectrum



(b) Northridge earthquake measured at Newhall

Fig. 7 Acceleration time history of earthquake waveforms used in this study (peak ground acceleration, PGA, scaled to 0.5 g)

Table 1 Static shear test results for unreinforced anchors

Specimen	V_{test} (kN)	u_{test} (mm)
ST-UN-01	63.1	3.3
ST-UN-02	56.8	2.5
ST-UN-03	62.7	2.8
ST-UN-04	60.3	3.2
Mean	60.7	3.0

4. Experimental results

4.1 Test results

Tables 1-2 presents the results of the static shear tests. The load–displacement curves of unreinforced and hairpin-reinforced anchors ST-UN-01 and ST-UH-01, respectively, are shown in Fig. 8. The unreinforced anchor exhibited no further load increase after cracking appeared around the anchor. In contrast, after cracking appeared around the hairpin-reinforced anchor (denoted as “first failure”), the load temporarily decreased. Then, as cracking progressed, the hairpin steel resisted the loading, and finally, the hairpin (or anchor) failed (denoted as “second failure”).

In the shaking table tests, the load and displacement at concrete breakout failure was determined for each specimen using the load and displacement measured at the anchor and the strains measured by the strain gauges on the shaft of the anchor and the surface of the concrete

Table 2 Static shear test results for hairpin-reinforced anchors

Specimen	1 st failure		2 nd failure	
	$V_{1,test}$ (kN)	$u_{1,test}$ (mm)	$V_{2,test}$ (kN)	$u_{2,test}$ (mm)
ST-UH-01	74.1	3.7	74.9	20.4
ST-UH-02	90.2	4.7	96.7	38.2
ST-UH-03	76.4	5.4	81.0	24.7
ST-UH-04	78.9	4.4	80.8	18.8
Mean	79.9	4.6	83.4	25.5

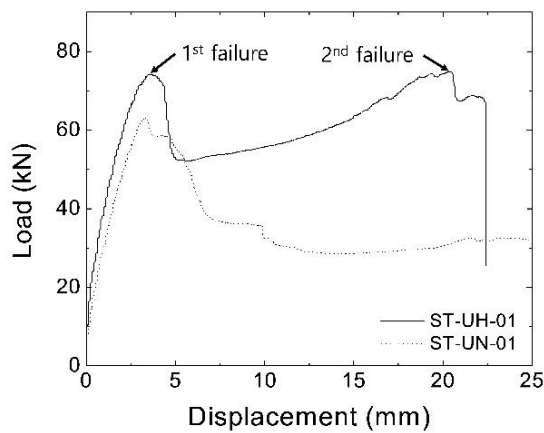


Fig. 8 Example of load-displacement curve from static shear test

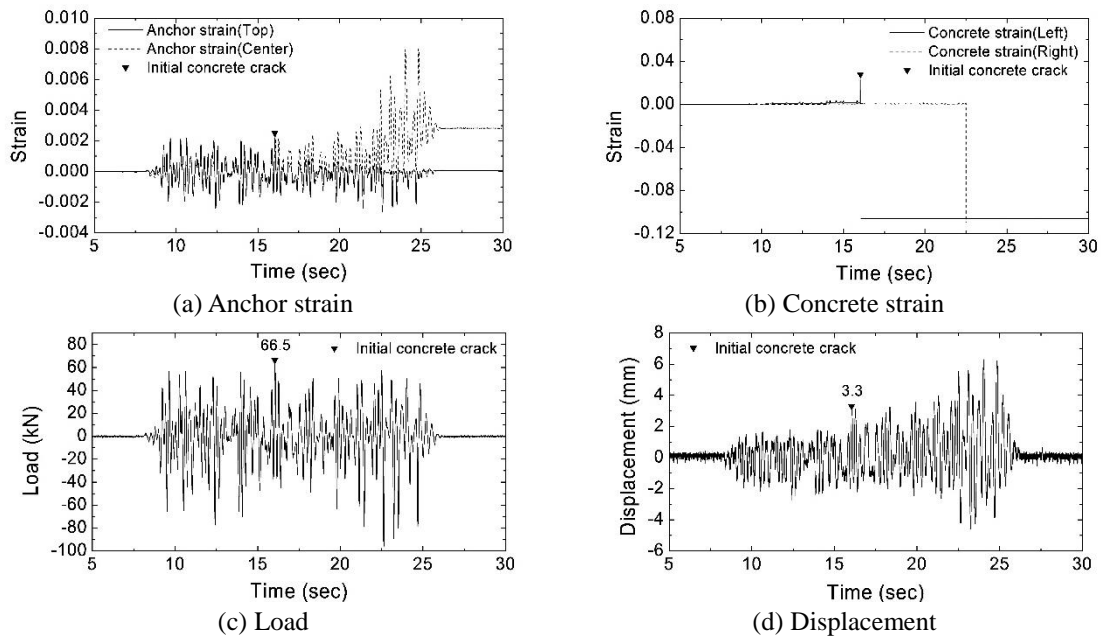


Fig. 9 Time histories of anchor strain, concrete strain, load, and displacement for SK-UN-01 specimen for US NRC artificial earthquake with PGA=0.30 g at failure

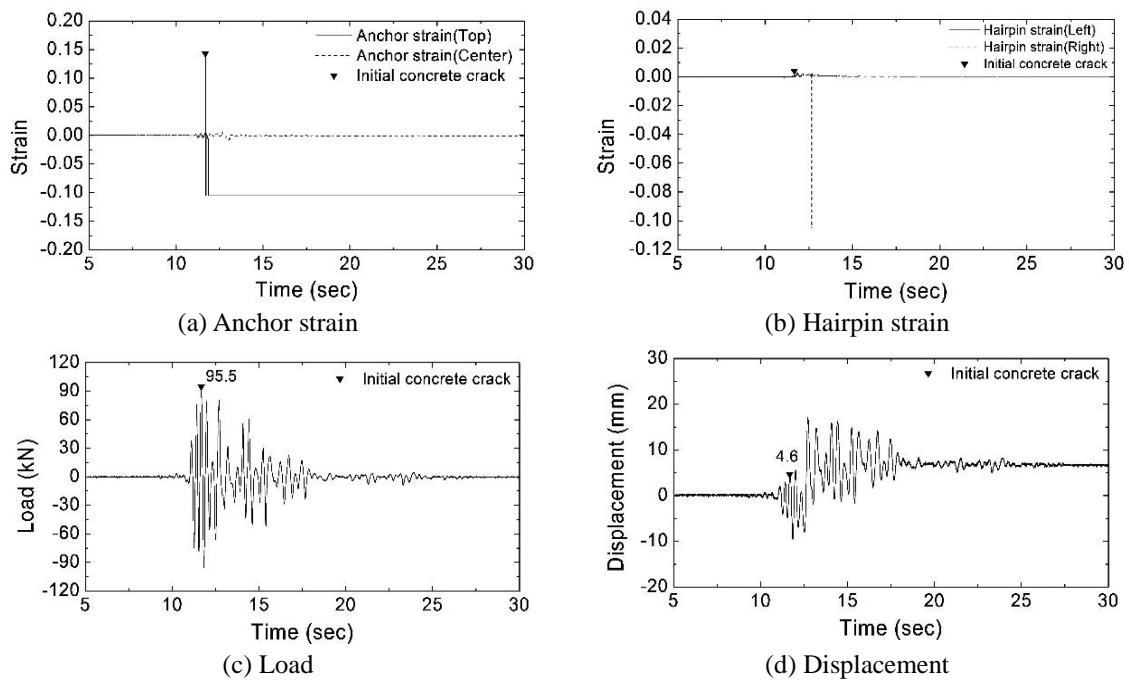


Fig. 10 Time histories of anchor strain, hairpin strain, load, and displacement for SK-UH-03 specimen for Northridge earthquake with $PGA=0.45$ g at first failure

block. Figs. 9-10 show examples of the variation in the measurements for the unreinforced and hairpin-reinforced anchors, respectively, at concrete failure.

Breakout failure of the concrete occurred due to positive (+) loading, i.e., loading in the edge direction, which produced tensile stress in the concrete. As shown in Figs. 9-10, microcracking was detected from the variation in the strains measured on the surface of the concrete block before the failure of the anchor but was not visible to the human eye. After the occurrence of microcracking, sudden fracture of the concrete was observed. Upon concrete fracture, the unreinforced (UN) anchor specimens exhibited large increases in displacement without any further resistance to loading, as shown in Figs. 9(c)-(d). For the hairpin-reinforced (UH) anchor specimens, the failure patterns for the US NRC seismic specimens (SK-UH-01 & 02) were different from those for the Northridge seismic specimens (SK-UH-03 & 04). The failure patterns of the latter two specimens were similar to the results of the static tests (see Fig. 11(a)), in which the final failure occurred due to steel fracture, accompanied by progressive cracking after the first failure of the concrete (see Fig. 11(b)). The failure patterns of the former two specimens indicated that crushing of the concrete occurred around the anchor and subsequent failure due to fatigue of the anchor before the hairpin failure (see Fig. 12). This fatigue failure might be attributable to the many peak loadings in the US NRC seismic waves.

Tables 3-4 summarize the PGAs, loads, and displacements for the unreinforced and reinforced anchors at failure. For the two types of seismic waves, which were not very different, the average concrete breakout strength was approximately 65.1 kN for the UN specimens. The average first failure strength for the four specimens with hairpin-reinforced anchors was 88.6 kN, and the average second failure strength, excluding SK-UH-01 and -02, was 95.6 kN.

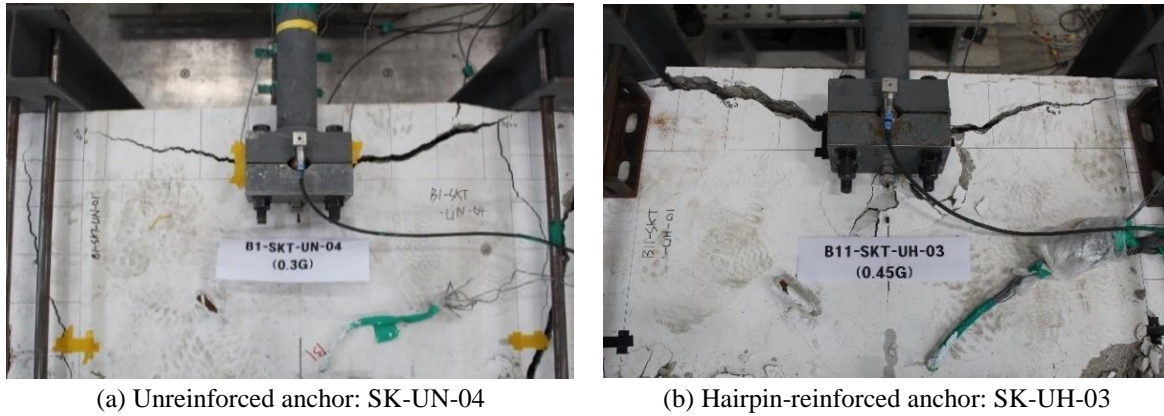


Fig. 11 Fracture shapes for unreinforced and hairpin-reinforced anchors

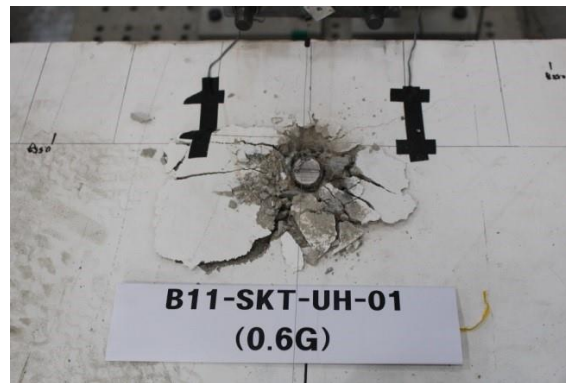


Fig. 12 Fracture failure of anchor shaft : SK-UH-01

Table 3 Shaking table test results for unreinforced anchors

Specimen	Earthquake	PGA (g)	V_{test} (kN)	u_{test} (mm)
SK-UN-01	US NRC	0.3g	66.5	3.3
SK-UN-02		0.3g	64.2	4.0
SK-UN-03	Northridge	0.3g	70.9	3.8
SK-UN-04		0.3g	58.9	3.3
Mean			-	65.1

4.2 Fracture shape

After the seismic tests were completed, the breakout shape of the concrete for the unreinforced and hairpin-reinforced anchors (see Figs. 11(a)-(b)) was measured. The right and left angles on the failed surface of the concrete and the side angle of the fracture at the anchor are shown in Fig. 13 as examples. Table 5 summarizes the fracture angles measured for each specimen. The hairpin-reinforced anchor specimens, SK-UH-01 and SK-UH-02, which failed due to failure of the steel anchor, as shown in Fig. 12, were excluded.

Table 4 Shaking table test results for hairpin-reinforced anchors

Specimen	Earthquake	1 st failure			2 nd failure		
		PGA(g)	$V_{1,test}$ (kN)	$u_{1,test}$ (mm)	PGA(g)	$V_{2,test}$ (kN)	$u_{2,test}$ (mm)
SK-UH-01*	US NRC	0.5g	87.7	3.6	0.55g	93.7	-
SK-UH-02*		0.45g	76.2	5.5	0.55g	94.8	-
SK-UH-03	Northridge	0.45g	95.5	4.6	0.5g	98.4	19.6
SK-UH-04		0.45g	94.8	4.6	0.5g	92.8	20.0
Mean		-	88.6	4.6	-	95.6**	19.8

* The specimens finally failed due to the fracture of anchor prior to the failure of hairpin.

** The average of SK-UH-03 and SK-UH-04 except for SK-UH-01 and SK-UH-02

Table 5 Surface fracture angles and breakout depths

Specimen	Reinforcement	Top surface (°)			Side surface (°)		Breakout depth(mm)	
		Left	Right	Mean	Angle	Mean	Depth	Mean
SK-UN-01	No reinforcement	12	18	19.3	56	57.5	105	110
SK-UN-02		24	33		54		120	
SK-UN-03		19	16		63		90	
SK-UN-04		14	18		57		124	
SK-UH-03	Hairpin reinforcement	23	18	25.5	67	57.5	153	181
SK-UH-04		21	40		48		209	

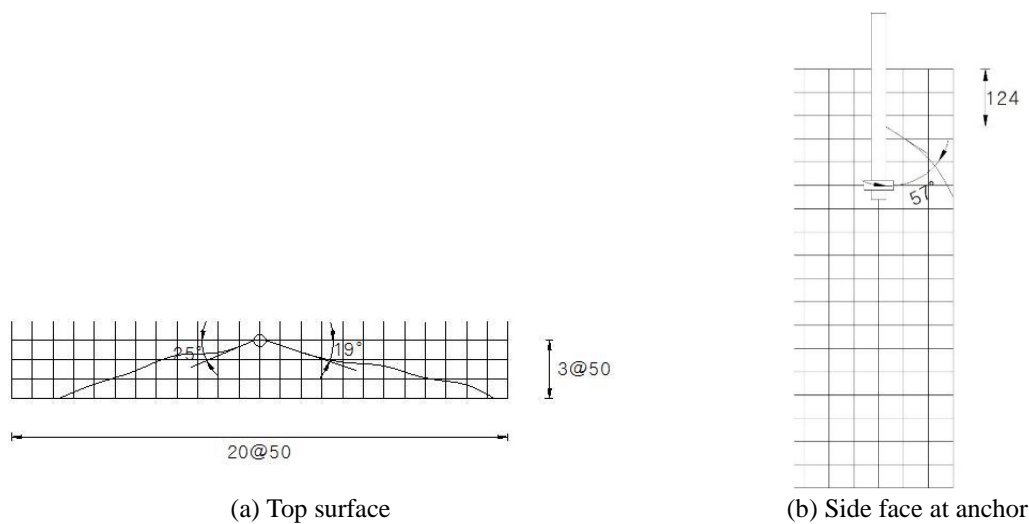


Fig. 13 Examples of fracture angles of the specimen SK-UN-04

The average angle on the top surface of the fracture was 19.3° for the unreinforced anchors and 25.5° for the hairpin-reinforced anchors. As in previous research (Lee *et al.* 2010) on the static shear resistance of concrete anchors, the fracture angle on the top surface was slightly lower than the idealized fracture angle of 35° in the CCD theory.

The depth of fracture was also measured, as shown in Fig. 13(b). For the UN specimens, the average depth was 110 mm, or 3.7 times the anchor diameter. For the UH specimens, the average depth was 181 mm, or 6.0 times the anchor diameter. The fracture depth of the UH specimens was thus approximately 1.6 times that of the UN specimens. According to the current design standards (Eq. (1)), the load-bearing length is taken to be a maximum of 8 times the anchor diameter, but the experimental results showed that the fracture depth could not reach the load-bearing length specified by the design standards, especially for the unreinforced anchors. The influence of the fracture depth on the concrete breakout strength is addressed in Section 5. The fracture angles and breakout depths obtained from static shear tests of unreinforced and hairpin-reinforced anchors were similar to those obtained from the shaking table tests.

5. Results and discussion

The concrete breakout strength depends mainly on the strength of the concrete. The average measured compressive strength of the concrete used in this study was 25.3 MPa. The effective area of D10 hairpin steel is 71.33 mm², and the yield and tensile strengths of the hairpin were 502 MPa and 624 MPa, respectively.

5.1 Comparisons of the seismic shear strength with the design strength for unreinforced anchors

Table 6 compares the average concrete breakout strengths obtained from the shaking table tests and static tests with those calculated using Eqs. (1)-(2) and (4), provided in ACI 318-02, ACI 318-11, and ETAG 001, respectively. In computing the design strength value, the load-bearing length was taken to be $l_e = 8d_o$. ACI 318 uses the cylinder strength (f_{ck}), whereas ETAG 001 uses the cube strength (f_{cc}). In this study, cube strengths were converted to cylinder strengths using the relation $f_{cc} = 1.18 f_{ck}$.

The mean concrete breakout strength obtained from the shaking table tests was 65.1 kN, which is 77%, 101%, and 95% of the strengths calculated from ACI 318-02, ACI 318-11, and ETAG 001 with $k = 3.0$, respectively. For comparison with the experimental results, the reduction factor of 0.75 stipulated in ACI 318-02 (to ACI 318-08) was not included in the calculation. The design standard of ACI 318-11 and ETAG 001 are in good agreement with the measurement, but ACI 318-02 overestimates the measured concrete breakout strength by approximately 23%.

Eq. (1) from ACI318-02 accounts for the effectiveness of the bearing length through the

Table 6 Comparisons of shear strengths from shaking table tests, and design standards for unreinforced anchors

Specimen	Loading	V_{test}^{mean} (kN)	ACI 318			ETAG 001	
			$V_{ACI318-02}^{l_e=8d_o}$ (kN)	$V_{ACI318-11}$ (kN)	$\frac{V_{test}^{mean}}{V_{ACI318-11}}$	$V_{ETAG001}^{l_e=8d_o}$ (kN)	$\frac{V_{test}^{mean}}{V_{ETAG001}}$
SK-UN-00	Seismic	65.1	84.4	64.7	1.01	68.9	0.95
ST-UN-00	Static	60.7			0.94		0.88
$V_{dyn.}/V_{static}$		1.07					

exponent of 0.2, and Eq. (4) from ETAG 001 accounts for it through the β exponent. Given the value $\beta=0.0725$ obtained for the data from this study, ETAG 001 appears to greatly mitigate the influence of this factor. In contrast, the revised Eq. (2) from ACI 318-11 does not account for the effects of the anchor diameter and the bearing length of the anchor. As described in Section 4.2, the measured failure depth of $3.7d_0$ did not approach $8d_0$. Therefore, the CCD strength indicated by Eq. (1) from ACI 318 could greatly overestimate the shear strength.

Table 6 shows that the average dynamic strength was approximately 7% greater than the static strength. This might be attributed to the effect of the strain rate, as discussed in Section 5.3. Therefore, the current standards, which equate the dynamic strength to the static strength of the unreinforced anchor, are suitable for use in design and incorporate some degree of safety.

5.2 Comparisons of the seismic shear strength with the design strength for hairpin-reinforced anchors

The revision of ACI 318-08 included a regulation that replaced the breakout strength of concrete with the strength of the steel reinforcement. The design strength of the hairpin steel, determined using Eq. (3), without considering the strength reduction factor (ϕ), was 71.6 kN ($= A_{se}f_y = 2 \times 71.33 \text{ mm}^2 \times 502 \text{ MPa}$), based on the yield strength of the steel, and 89.0 kN ($= A_{se}f_u = 2 \times 71.33 \text{ mm}^2 \times 624 \text{ MPa}$) based on the tensile strength of the steel.

ETAG 001 does not provide a specification for steel reinforcement. Therefore, the first and second failures in the shaking table and static shear tests were compared with ACI 318 only, as shown in Table 7. Eq. (3) from ACI 318 does not distinguish between the first and second failures for hairpin reinforcement and takes the yield strength of the steel to be the shear strength of a hairpin-reinforced anchor, without considering the shear resistance of the concrete. However, the authors' opinion is that this is necessary to distinguish between the first and second failures and thus determine the ultimate strength of hairpin-reinforced anchors.

Fig. 14 illustrates the hairpin strain of the ST-UH-03 specimen before and after the first failure. The hairpin strain occurred on the verge of cracking of the concrete and rapidly increased after the concrete cracked. This means that the concrete and the reinforcing steel both resisted the first failure. According to Tables 6-7, the average static strengths of the unreinforced and hairpin-reinforced anchors were 60.7 kN and 79.9 kN, respectively. The influence of the hairpin resistance effect, V_{hp} , can be calculated using the following equation proposed by Eligehausen *et al.* (2006):

$$V_{hp} = nA_{se}f_y \tag{5}$$

where n is the effectiveness index. The effectiveness index of the hairpin is $(79.9 \text{ kN}-60.7 \text{ kN})/71.6 \text{ kN}=0.27$. For dynamic loading, as with the increase in strain before the first failure, the effectiveness index of the hairpin is $(88.6 \text{ kN}-65.1 \text{ kN})/71.6 \text{ kN}=0.33$ (see Tables 6-7).

At the second failure, the hairpin only provided resistance after the concrete breakout cone had formed completely. Therefore, it is reasonable that the strength of the hairpin be taken as that of the second failure. According to Table 7, the average static strength (83.4 kN) was greater than the yield strength of the hairpin (71.6 kN) and less than the ultimate strength (89.0 kN). Therefore, the second failure strength of the hairpin-reinforced anchor is safe and appropriate for use as the strength of the steel according to the current ACI 318 standard. However, the current ACI 318 standard only accounts for the strength of the steel, as explained previously, and this would be not economical when the first failure strength is greater than the second failure strength. Therefore,

Table 7 Comparisons of shear strengths from shaking table tests, static tests, and design standards for hairpin-reinforced anchors

Specimen	Loading	1 st failure			2 nd failure		
		$V_{1,test}^{mean}$ (kN)	$V_{ACI318-11}$ (kN)	$\frac{V_{1,test}^{mean}}{V_{ACI318-11}}$	$V_{2,test}^{mean}$ (kN)	$V_{ACI318-11}$ (kN)	$\frac{V_{2,test}^{mean}}{V_{ACI318-11}}$
SK-UH-00	Seismic	88.6	71.6	1.24	95.6	71.6	1.34
ST-UH-00	Static	79.9		1.12	83.4		1.16
$V_{dyn.}/V_{static}$		1.11			1.15		

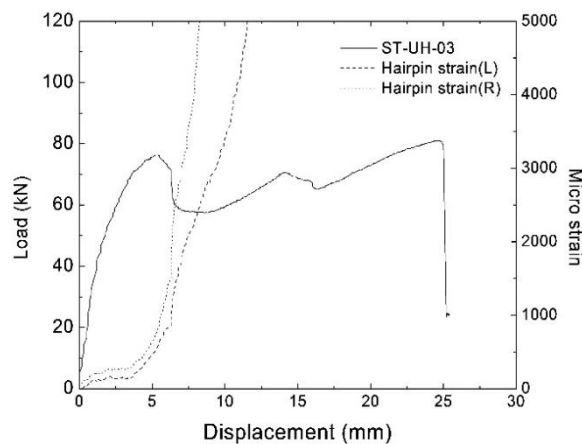


Fig. 14 Hairpin strain of ST-UH-03

supplementary tests that take into account the edge distance of the anchor and the parameters of the hairpin need to be performed to distinguish between the first and second failure strengths.

The dynamic strength of the hairpin-reinforced anchor increased by 11% for the first failure and 15% for the second failure as shown in Table 7. This might be due to the strain rate effect of the steel, as discussed in Section 5.3. Therefore, the current standard, which equates the dynamic strength of a steel-reinforced anchor to its static strength, can be expected to provide safe results in design.

5.3 Analysis of the load frequency and strain rate

A fast Fourier transform was performed to analyze the load frequency for the SK-UN-03 (Northridge seismic wave) and SK-UH-02 (US NRC seismic wave) specimens, as illustrated in Fig. 15. As with the other specimens, the principal frequency was in the range of 3-4 Hz.

Tables 8-9 present the strain rates of the concrete and hairpin from the shaking table tests. The strain rate of the concrete was analyzed for the unreinforced and hairpin-reinforced anchors at the maximum load before the concrete cracked. The strain rate of the hairpin anchors was analyzed before and after the concrete cracked at the first failure. According to Table 8, the average strain rates of the concrete in the UN and UH specimens were 5.14×10^{-2} and 5.35×10^{-2} , respectively, which are both within the range of 10^{-3} to 10^{-1} . Pajak (2011) collected test data to assess the dynamic increase in the tensile strength as a function of the concrete strain rate, as illustrated in

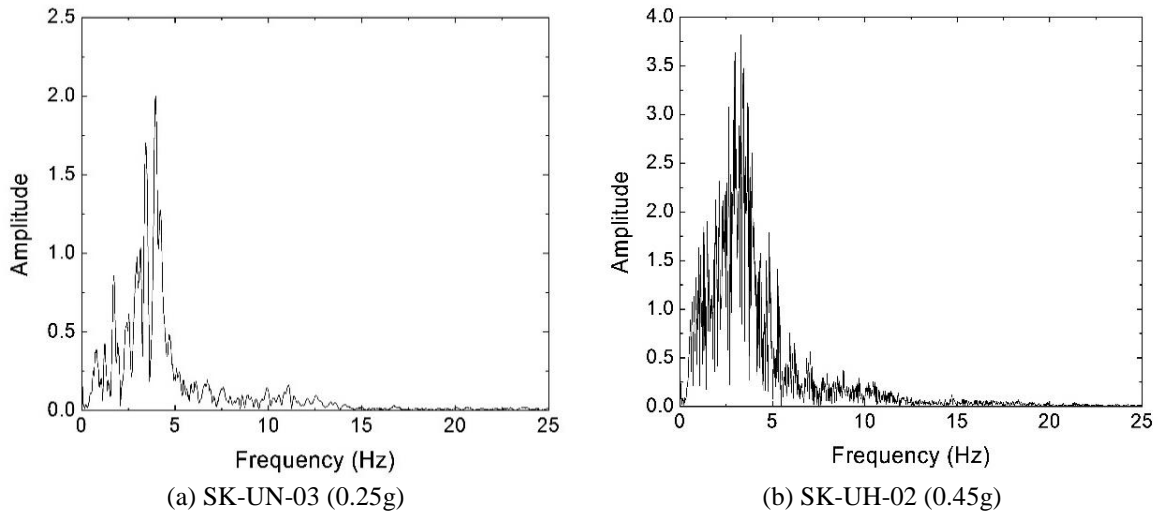


Fig. 15 Loading frequency (shaking table test)

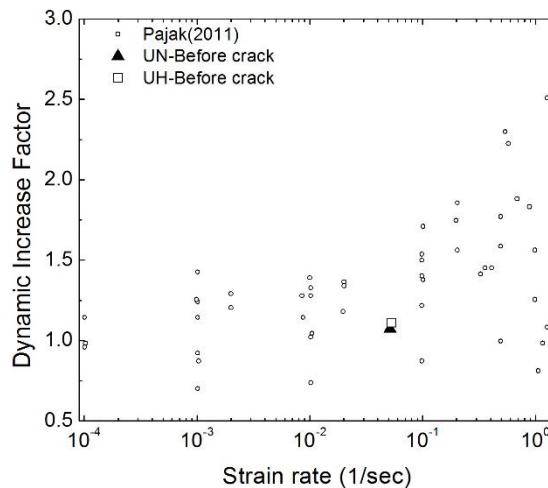


Fig. 16 Average strain rate of concrete (shaking table test)

Fig. 16. The average strain rate obtained in this study was in the range of the dynamically increased strength. The dynamic strength increases of 7% for the unreinforced anchor and 11% (to first failure) for the hairpin-reinforced anchor can be explained by the strain rate effect.

The average strain rate of the hairpins was 3.09×10^{-2} before concrete cracking and 1.04×10^{-1} after concrete crack at the first failure. Malvar (1998) presented data on the dynamic increase in the yield strength of steel, as illustrated in Fig. 17. The average hairpin strain rate obtained in this study was also in the range of the dynamically increased strength. The dynamic strength increases of the hairpin-reinforced anchor of 11% at the first failure and 15% at the second failure can also be explained by the strain rate effect.

As a result, the shaking table test results showed no reduction in the dynamic shear strengths of unreinforced and hairpin-reinforced anchors. Compared to the static strength, the dynamic strength

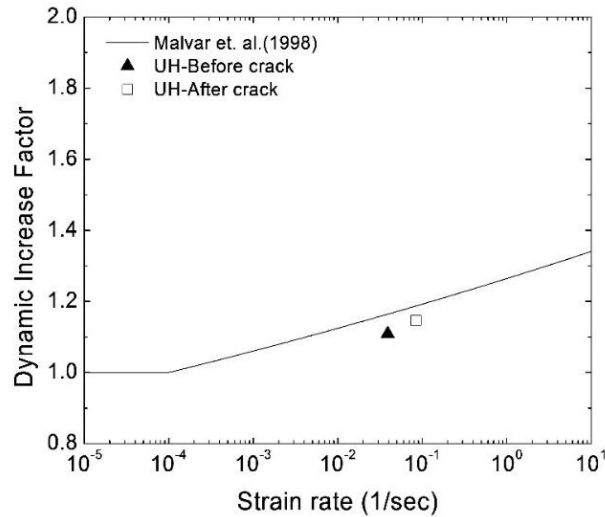


Fig. 17 Average strain rate of hairpin (shaking table test)

Table 8 Strain rate (1/s) of concrete for unreinforced and hairpin-reinforced anchors before concrete cracking

Specimen	Concrete strain rate		Specimen	Concrete strain rate	
	Left	Right		Left	Right
SK-UN-01	1.0727E-01	3.1234E-02	SK-UH-01	6.9124E-03	4.8131E-02
SK-UN-02	2.6370E-02	6.9124E-03	SK-UH-02	2.3297E-02	2.4578E-02
SK-UN-03	5.0947E-02	3.8393E-02	SK-UH-03	1.1393E-01	1.1930E-01
SK-UN-04	1.0212E-01	4.8131E-02	SK-UH-04	8.4997E-02	6.6564E-03
Mean	5.14E-02		Mean	5.35E-02	

Table 9 Strain rate (1/s) of hairpin for hairpin-reinforced anchor before and after concrete cracking

Specimen	Hairpin strain rate: before crack		Hairpin strain rate: after crack	
	Left	Right	Left	Right
SK-UH-01	2.5858E-02	1.9201E-02	2.7898E-02	2.9954E-02
SK-UH-02	1.9201E-02	1.3569E-02	2.5090E-02	2.2017E-02
SK-UH-03	3.5586E-02	6.9893E-02	1.1188E-01	gauge out
SK-UH-04	5.5812E-02	7.2965E-02	4.0783E-01	gauge out
Mean	3.90E-02		1.04E-01	

was slightly higher due to the effect of the strain rate. However, in the anchor joint, at a lower frequency than the forcing frequency used in this study (3-4 Hz), the increase in the dynamic strength would be minor or negligible because the strain rate would be smaller. Therefore, the dynamic strength of unreinforced and reinforced anchors under earthquake loading could reasonably be estimated to be the same as the static strength.

6. Conclusions

The dynamic shear strengths of unreinforced and hairpin-reinforced anchors were evaluated in this study using shaking table tests. The main conclusions from this study are as follows:

- The CCD strength according to ACI 318-02, which is very sensitive to the load-bearing length, overestimates the static and dynamic shear strengths when the maximum length of $8d_o$ proposed in the code is considered. In contrast, the shear strengths calculated according to ETAG 001, which takes into account the effect of the load-bearing length to a lesser degree than ACI 318-02, and according to ACI 318-11, which does not take the effect of the load-bearing length into account at all, were close to the experimental values.
- The failure of the hairpin-reinforced anchors in the shaking table tests distinguished between the first failure (due to concrete failure) and second failure (final failure due to steel failure). ACI 318, however, neglects the resistance of the concrete and applies the yield strength of the hairpin only for the reinforced anchor. It is acknowledged that the second failure strength can be reasonably calculated using the yield strength of the steel. However, in estimation of the first failure strength, it would be reasonable to add the contribution of the resistance of the steel to the resistance of the concrete. Supplementary tests that take into account the edge distance of the anchor and the parameters of the hairpin need to be performed for this purpose.
- The dynamic strength of the unreinforced anchors as determined from the shaking table tests were 7% higher than the static strength. The dynamic first and second failure strengths of the hairpin-reinforced anchors were 11% and 15% greater, respectively. The results showed no reduction in the dynamic strength. The increase in strength can be explained by the strain rate effect of concrete and steel. However, the increase in the dynamic strength would decrease in the anchor joint as the loading frequency became lower than the forcing frequency (3-4 Hz) used in the shaking table tests in this study.
- The results of the shaking table tests, as an initial study on the shear strength of anchors using the seismic wave, indicated that the static shear strength could be used for the dynamic shear strength of anchors. Thus, the revision of ACI 318-11, which removed the strength reduction factor for the shear strength of anchors under an earthquake, could be reasonable. However, the experiment involved in this study was carried out for the case of the forcing frequency in the range of 3 to 4 Hz. Thus, a future study for the different frequency range would be needed to evaluate the dynamic shear strength of anchor, as well as the strain effect of concrete and anchor.

Acknowledgments

This work was financially supported by the National Research Foundation of Korea (Research Project No. 2013R1A2A2A01013872).

References

- ACI Committee 318 (2002), Building Code Requirements for Structural Concrete and Commentary, ACI 318-02, Appendix D: Anchoring to concrete, American Concrete Institute.
- ACI Committee 318 (2008), Building Code Requirements for Structural Concrete and Commentary, ACI

- 318-08, Appendix D: Anchoring to concrete, American Concrete Institute.
- ACI Committee 318 (2011), Building Code Requirements for Structural Concrete and Commentary, ACI 318-11, Appendix D: Anchoring to concrete, American Concrete Institute.
- ACI Committee 318 (2014), Building Code Requirements for Structural Concrete and Commentary, ACI 318-14, Chap. 17 Anchoring to concrete, American Concrete Institute.
- ACI Committee 349 (2001), Code Requirements for Nuclear Safety Related Concrete Structures (ACI 349-01); Appendix B Anchoring to Concrete, American Concrete Institute.
- ACI 355.2 (2000), Evaluating the Performance of Post-installed Mechanical Anchors in Concrete, Reported by ACI Committee 355.
- CSA N287.2 (1998), Material Requirements for Concrete Containment Structures for CANDU Nuclear Power Plants, Canadian Standards Association, Rexdale, Ontario.
- Eligehausen, R. and Hofmann, J. (2003), "Experimental and numerical investigation on fixings under shear loading close to an edge", Report, Institute of Construction Materials, University of Stuttgart. (in German)
- Eligehausen, R., Mallee, R. and Silva, J.F. (2006), *Anchorage in Concrete Construction*, Ernst & Sohn, Germany.
- ETAG 001 (2012), Guideline for European Technical Approval of Metal Anchors for Use in Concrete, European Organization for Technical Approvals (EOTA).
- Gross, J.H., Klingner, R.E. and Graves III, H.L. (2001), "Dynamic anchor behavior of single and double near-edge anchors loaded in shear", *Proc. of Connections between Steel and Concrete, Int. Conference organized by University of Stuttgart*, fib, IABSE, Ed. R. Eligehausen, RILEM Publications S.A.R.L.
- Klingner, R.E., Mendonca, J.A. and Malik, J.B. (1982), "Effect of reinforcing details on the shear resistance of short anchor bolts under reversed cyclic loading", *ACI J.*, **79**(1), 3-12.
- Lee, N.H., Park, K.R. and Suh, Y.P. (2010), "Shear behavior of headed anchors with large diameters and deep embedments", *ACI Struct. J.*, **107**(4), 146-156.
- Malvar, L.J. and Crawford, J.E. (1998), "Dynamic increase factors for steel reinforcing bars", *Proc. of the Twenty-Eighth DDESB Seminar*, Orlando, Florida.
- Pajak, M. (2011), "The influence of the strain rate on the strength of concrete taking into account the experimental technique", Architecture Civil Engineering Environment, The Silesian University of Technology.
- Park, Y.M., Kang, M.K., Roh, J.K., Ju, H.J. and Kang, C.H. (2014), "Shear resistance of CIP anchors under dynamic loading: Reinforced anchor", *J. Korean Soc. Steel Constr.*, **26**(1), 21-31. (in Korean)
- Petersen, D., Lin, Z. and Zhao, J. (2013), "Behavior and design of cast-in-place anchors under simulated seismic loading", Draft Final Report, Vol. 1, Cyclic Behavior of Single Headed Anchors, Department of Civil Engineering, University of Wisconsin, Milwaukee.
- US NRC Regulatory Guide 1.60 (1973), Design response spectra for seismic design of nuclear power plants, United States Nuclear Regulatory Commission, Washington.